Competing phases in a dilute magnetic semiconductor layer model with magnetic polaron formation

M. Kiselev[1], R. Oppermann[1,2], D. Sherrington[2]
[1] *Institut für Theoretische Physik, Universität Würzburg, 97074 Würzburg, F.R.Germany*
[2] *Department of Physics, University of Oxford, 1 Keble Road, Oxford OX1 3NP, U.K.*
(May 30, 2000)

dedicated to the 60th birthday of Franz J. Wegner

The magnetic phase diagram of a layered II-VI semiconductor model with s-d coupling between interface-localized exciton holes and the magnetic layer is analyzed. As a function of three competing interactions, which can be varied experimentally, we find various sequences of thermal transitions between maximally four different types of magnetic order and a classical phase transition at $T = 0$. A sudden breakdown of the magnetic polaron and its restoration at higher temperature is found to occur for a certain parameter regime. The competition between spin glass and antiferromagnetic order and the polaron-size determine predominantly existence and shape of the polaron depression. Previous work done on a $CdTe/Cd_{1-x}Mn_xTe$ Villain-pseudospin model is generalized in many directions, which includes i) magnetic field behaviour, ii) regime of replica symmetry breaking by calculation of an Almeida Thouless surface, iii) effects of antiferromagnetic interaction in the magnetic layer, iv) polaron size effects, and, above all, v) an exploration of the whole range of magnetic phenomena and limitations of the model.

I. INTRODUCTION

Advances in nanostructuring of materials appears to lead to rapidly growing possibilities for comparing theory with experiments on systems which show on one hand true phase transitions but also mesoscopic size effects and dimensional crossover.

In pioneering papers mesoscopic effects were considered by Weissman[1,2] as a tool for understanding complex magnetism such as spin glass order. Weissman dealt with the fundamental question of whether the droplet picture or Parisi symmetry breaking provide a proper description of experimental facts. More recently, other groups[3,4] analyzed for example conductance noise of mobile carriers which experience scattering on randomly frozen magnetic moments. Moreover, citing here only a few different examples, an analogy with 1/f noise was observed in conductance fluctuations and discussed by Dietl et al[3].

In previous work[5] we adapted an SK-type Villain Ising pseudospin-model[6] to a finite size and mesoscopic problem of layered II-VI dilute magnetic semiconductor (DMS). Quantitative and qualitative agreement with experiments was achieved by the calculation of the magnetic part of the exciton magnetic polaron energy and of the Zeeman splitting. An optimal fit with experimental data for a particular sample $Cd_xMn_{1-x}Te$, $x = 33\%$, was obtained and proved the need for the presence of spin glass order parameters and small antiferromagnetic clusters. Simpler descriptions in terms of Brillouin functions employing Neél-temperature shifts, as borrowed from antiferromagnetic systems, were incompatible with specific features of the experimental data[5].

In this earlier work, magnetic field dependence, replica symmetry breaking, and the attempt to model the antiferromagnetic effects by an explicit antiferromagnetic interaction in the Hamiltonian were not yet considered. This will be achieved in the present paper and, in addition, the present work is geared to provide a general view of the physics of the multi-parameter DMS layer model with substantial polaron formation. We consider this theoretical work suitable to stimulate further experiments and an indispensable condition for a cross-control with predictions of alternative Heisenberg model descriptions or QMC calculations.

In this respect the role of the Heisenberg nature of manganese spins is important, since Rigaux et al[7] showed the existence of a Gabay-Toulouse line in the magnetic field behaviour. The anisotropy induced by a Dzyaloshinskii-Moriya interaction may be responsible for Ising behaviour.

Our model is analyzed without imposing restrictions on the many parameters which determine its phases and the transitions between them. A rather involved picture emerges as a function of three competing interactions, of the finite polaron partition of the magnetic CdMnTe–layer, and of the number of polaron spins associated with each of the independent exciton-holes.

Several motivating aspects for further research existed since Ref. 5. For example the need to include small antiferromagnetic clusters in order to obtain an optimal fit suggests to give up full frustration in favor of partial frustration

with additional antiferromagnetic interaction. This is also required to describe the antiferromagnetic phase transition which is known to occur[8] at high manganese concentration x.
Corrections of replica symmetry breaking have been shown to become large at low temperatures. They play a fundamental role in spin- and fermionic systems as well. Their experimentally verifiable role is interesting in itself. For example the phenomenon of (history-dependent) aging[10] appears to require Parisi replica symmetry breaking (RSB). The goal of the present work is to meaning and the limitations of replica symmetric results under the participation of frustrated, of antiferromagnetic and of s-d mediated interactions.

II. THE VILLAIN PSEUDOSPIN MODEL FOR EXCITON HOLE GENERATED POLARONS IN DMS LAYERS

Magnetic properties of the semimagnetic semiconductor $(Cd,Mn)Te$ are determined by the spin$5/2$ Mn^{2+} ions that substitute Cd-ions randomly in the geometrically frustrated fcc lattice. The Pauli exclusion principle allows such a redistribution of electrons of the d-shell of Mn^{2+}-ion such that the total spin of electrons attains its maximal possible value $S = 5/2$, whereas the total orbital momentum sums up to zero. The interaction between the band of (s or p)-electrons and localized d-moments can be cast in the usual $s-d$ exchange form. The interaction between local moments is mediated by conduction electrons through Ruderman-Kittel-Kasuya-Yosida (RKKY) exchange and results in effectively antiferromagnetic coupling. The strength of the antiferromagnetic interaction between Mn-spins falls off rapidly with the distance. Thus, the nearest neighbour (NN) approximation can be used instead of long range RKKY-exchange. By increasing the manganese concentration, clusters of magnetically coupled Mn ions are formed. At concentration above 20% a percolating Mn cluster emerges, which exibits a transition into a spin glass phase.
In Ref. 5 the Ising pseudospin model of a spin glass was proposed for $(Cd,Mn)Te$. According to this model the magnetic entity that freezes at low temperatures is not a Heisenberg Mn spin, but a tetrahedron with four Mn-spins on the top. Such tetrahedrae are formed at high enough concentration of Mn. Due to antiferromagnetic next-neighbour interaction, the Mn spins in the ground state of the tetrahedron build so-called canted structures. All ground state configurations of the tetrahedron can be divided into two classes, providing that the configurations from different classes can not be transformed one into another by a continuous rotation of spins. Each class can be characterized by a topological invariant $\xi_{ijk} = \sigma_i(\sigma_j \times \sigma_k)$ that is a mixed product of three spins from any face of the tetrahedron. The normalized value $S = \xi/|\xi|$ can be considered as an Ising pseudospin.
In an earlier paper[5] we focussed on the explanation of experiments performed on a $CdTe/Cd_{1-x}Mn_xTe$ layered system with $x = .33$ by means of a frustrated Villain-pseudospin model. It was possible to fit all specific features, which could not be explained before by apparently oversimplified models.
The given concentration of manganese implies a freezing temperature of roughly $8K$ at $x = .33$. This phase was analyzed in our paper[5] by the use of spin glass order and in a replica symmetric approximation. The basic feature such as a maximum in the magnetization and corresponding EMP energy was generated by our model in agreement with the experiment.
The intention of the present paper is to derive all relevant cornerstones of the general phase diagram that occurs under variation of the manganese concentration. The theoretical model of Ref. 5 is extended in a way which allows partial frustration and the inclusion of a translationally invariant antiferromagnetic interaction. This is achieved by combining our exciton magnetic polaron model[5] with the Korenblit-Shender model of an antiferromagnetic spin glass[9]. The basic step is to define an interaction between two sublattices and to distribute the random part by a standard Gaussian weight function. Korenblit and Shender derived for such a model an Almeida Thouless line, which deviates remarkably from the ferromagnetic counterpart. The exciton magnetic polaron changes the behaviour in an external field and one is bound to reconsider the line of ergodicity breaking and, of course the complication of replica symmetry breaking beyond the line. The model extension is physically important, since not only the freezing temperature rises with increasing manganese concentration x but also the antiferromagnetic interaction part becomes larger.
The two-sublattice model we are analyzing in this paper is described by the Hamiltonian

$$\mathcal{H} = -\sum_{i_1=1}^{N_S}\sum_{j_2=1}^{N_S} J(r_{i_1}, r_{j_2})S(r_{i_1})S(r_{i_2}) - \frac{J_K}{2N_1}\sum_{l=1}^{N_p}\sigma(R_l)\sum_{i_1,i_2=1}^{N_1}[S(R_l + r_{i_1}) + S(R_l + r_{i_2})]$$
$$-H\sum_{l=1}^{N_p}\sum_{i_1,1_2=1}^{N_S}[\sigma(R_l) + S(R_l + r_{i_1}) + S(R_l + r_{i_2})] - \frac{1}{N_p}\sum_{l=1}^{N_p}\sum_{k=1}^{N_p} J_{h-h}\sigma(R_l)\sigma(R_{l+k}) - \sum_{l=1}^{N_p}\mu_h\, n(R_l), \qquad (1)$$

where r_{i_1}, r_{i_2} run over the sites of the distinct sublattices 1 and 2, respectively. We denote the Ising Villain-spins by S, representing thus tetrahedra of manganese Heisenberg spins by simpler effective pseudospins with only two

orientations[6], and the exciton hole spin at the interface-site R_l by $\sigma(R_l)$. The (ferromagnetic) exchange coupling with each of the N_p hole spin is restricted to a subset of N_1 among the N_S Villain spins. The concentration of exciton holes can in principle be controlled by a chemical potential μ, which may generalize too the previous model[5]. Each exciton hole forms one polaron. However, the number N_p of polarons should equal the hole number, which needs a selfconsistent calculation. We consider in most of the calculations of this paper $\mu_h = 0$. A low hole density is assumed such that polarons do not overlap. For this reason the hole-hole interacion J_{h-h} is considered to be very small and negligible in most of the calculations. If we speak about ferromagnetic alignment of polaron and hole-spins below a much higher polaron temperature (set by the s-d coupling J_K) this means that the transition is subject to fluctuation effects. Without any doubt the polaron temperature $T_p \sim J_K$ can be so high that one can speak of a pseudo-ferromagnetic phase; this was in fact the case in the $x = .33$ sample of $Cd_{1-x}Mn_xTe$[5].
The model definition is completed by the definition of a Gaussian distribution for the independent coupling constants (acting between different sublattices)

$$P(\delta J) = \sqrt{\frac{N_S}{2\pi}}\, exp\left[-\frac{N_S}{2}\frac{(\delta J + J_{af}/N_S)^2}{J^2}\right] \tag{2}$$

where $J(r_{i_\lambda}, r_{j_{\bar{\lambda}}}) = \delta J(r_{i_\lambda}, r_{j_{\bar{\lambda}}}) + J_{af}(r_{i_\lambda} - r_{j_{\bar{\lambda}}})$
Thermodynamic limit, phase transition, and mesoscopic feature: we illustrate the model by Figure 1

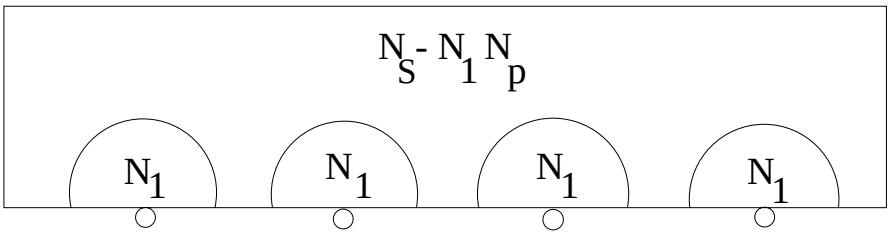

FIG. 1. Layer model with polarons of N_1 spins; each polaron (large semi-circle) belongs to one of N_p interface sites of exciton holes (small circles). The total number of spins not included in the polaron is indicated to be $N_S - N_p N_1$. All N_S spins interact equally via a partially frustrated interaction with antiferromagnetic part.

where the thermodynamic limit is reached by taking the number N_p of polarons and the total number of Villain spins N_S to infinity. The number of spins N_1 of each polaron is kept finite; numerically we consider the range of $N_1 \approx 10 - 100$. This is enough to find three-dimensional behaviour in the magnetic layer. Finite size effects then remain due to a factor $N_1 N_p/N_S$ which assumes finite values between 0 and 1. This spatial inhomogeneity introduces a third competing interaction based on $J_K > 0$ and hence with ferromagnetic tendency. Taking formally the number of polaron-spins N_1 to infinity, the hole polarization effect on the polaron spins becomes of measure zero (keeping fixed the s-d interaction) and one returns to the case of antiferromagnetism competing with spin glass order as considered by Korenblit and Shender[9].

III. THE COMPETITION BETWEEN PARTIALLY FRUSTRATED -, ANTIFERROMAGNETIC -, AND FERROMAGNETIC S-D INTERACTION WITH THE EXCITON HOLE

Korenblit and Shender[9] elaborated the difference between the ferromagnet-spin glass and the antiferromagnet-spin glass phase diagram as it emerges in an external magnetic field. An effective field like the one that exists within the magnetic polaron regime will prove to have a similar but more involved effect. Since the effective polaron field originates however in the s-d ferromagnetic interaction between exciton-hole spin and manganese spins, the multiple competition between direct and mediated interactions lead to a particularly rich phase diagram. This multiple competition exists between ferromagnetic s-d coupling, which leads to an effective polaron field, antiferromagnetic interaction of the manganese spins, and frustrated interaction which tends to freeze random order and thus competes with any kind of translationally invariant order. Moreover these interactions are confined within regions that possess only limited spatial overlap, depending on the extension of the polaron inside the magnetic system. The latter roughly corresponds to the extension of the exciton hole wave function within the magnetic layer.

Practically all coupling constants can be varied in the experiment. The strength of the s-d coupling depends on the interface, on the prelocalization of the excitons and on the manganese concentration too. At very low concentrations even a change of sign is expected, resulting in an antiferromagnetic s-d coupling and a Kondo effect that has its own specific way of competition with the spin glass phase. A true quantum phase transition must be expected there, but this is not subject of the present paper. The antiferromagnetic part of the Villain spin interaction clearly increases with the manganese concentration and eventually leads to the spin glass-antiferromagnet phase transition at high concentrations. Monte Carlo calculations were applied to this case in[8]. We consider this transition in the framework of the Villain pseudo Ising spin model below. Specific predictions from the present model give hints for future experiments.

A. Free energy and the set of selfconsisent equations: experimental relevance at low temperatures

Let us first report results within the replica symmetric approximation. In the simplest case already five coupled selfconsistent equations must be solved simultaneously, and, employing these solutions, the free energy has to be evaluated in order to determine the stable solution. This task becomes rather complicated at 1RSB, but several of the phase transitions occur outside the regime of broken ergodicity and, for the rest, the 0RSB is proved to be qualitatively right.
The free energy reads up to an irrelevant constant

$$\mathcal{F} = \frac{N_p}{N_S} J_K \; p \; M_p - J_{af} \; m_1 m_2 - \frac{J^2}{2T}(q_1 - 1)(q_2 - 1) - T\frac{N_1 N_p}{N_S} \sum_{\kappa=1,2} \int_{z_\kappa}^{G} ln \left[cosh(\tilde{H}_\kappa(p, z_\kappa)/T) \right]$$

$$-T\frac{N_S - N_1 N_p}{N_S} \sum_{\kappa=1,2} \int_{z_\kappa}^{G} ln \left[cosh(\tilde{H}_\kappa(0, z_\kappa)/T) \right] - T\frac{N_p}{N_S} ln \left[cosh((H + J_K M_p)/T) + cosh(\mu_h/T) \right] \tag{3}$$

where the effective field $\tilde{H}$ is different inside and outside the polaron. The total number of Villain spins S within the magnetic barrier is denoted by N_S, while the number of polarons is called N_p, and N_1 stands for the number of Villain-spins on each sublattice of a single polaron. The effective field on sublattices 1 and 2 is given by

$$\begin{aligned} \tilde{H}_1(p, z_1) &= H + J_K p/N_1 - J_{af} m_2 + J\sqrt{q_2}\; z_1 \\ \tilde{H}_2(p, z_2) &= H + J_K p/N_1 - J_{af} m_1 + J\sqrt{q_1}\; z_2 \end{aligned} \tag{4}$$

The selfconsistent equations follow as

$$p = tanh[\frac{H}{T} + \frac{J_K}{T} \left[\int_z^G tanh(\tilde{H}_1(p, z)/T) + \int_z^G tanh(\tilde{H}_2(p, z)/T) \right]] \tag{5}$$

$$m_\kappa = \alpha \int_z^G tanh(\tilde{H}_\kappa(p, z)/T) + (1 - \alpha) \int_z^G tanh(\tilde{H}_\kappa(0, z)/T) \tag{6}$$

$$q_\kappa = \alpha \int_z^G tanh^2(\tilde{H}_\kappa(p, z)/T) + (1 - \alpha) \int_z^G tanh^2(\tilde{H}_\kappa(0, z)/T) \tag{7}$$

where $\kappa = 1, 2$ and $\alpha \equiv \frac{N_1 N_p}{N_S}$. We have omitted a contribution from J_{h-h} due to the smallness of the coupling; its inclusion into the mean field equations would be obvious. Since we consider nonoverlapping polarons one can set the total number of spins N_S of the magnetic layer $N_S \equiv N N_p$ and thus remove the polaron number from the equations.

1. *Our strategy to obtain the general phase diagram by solving the multidimensional selfconsistency problem*

The number of model parameters N_1, N, J, J_K, J_{af}, and eventually μ_h together with variables temperature and magnetic field is too large to derive and represent without difficulty the general phase diagram. We take the satisfying fit of the Villain spin model with experiments for a given sample[5] and different models as a motivation and justification to consider the phase diagram in generality. We chose to analyze first the $T \to 0$ limit, since the multiple solutions depend on a smaller number of parameters and allow a classification and determination of the stable solution in a general way.

B. Zero temperature limit of the selfconsistent equations

The zero temperature limit of the multiparameter free energy and of the saddle point equations contain a welcomed reduction of the number of free parameters. The spin glass order parameter on both sublattices saturate, $q_1(0) = q_2(0) = 1$ while the hole polarization can be either $p = 1$ or $p = 0$, depending on the coupling constants.

1. The different magnetic phases at zero temperature and transitions between them

The considerable simplification of the large set of coupled equations at $T = 0$ helps in finding a cornerstone of the phase diagram. For either hole polarization $p = 0$ or $p = 1$ we find solutions, which allow for phase transitions, but also between the two classes transitions occur.

The zero temperature limit of the free energy reads (up to irrelevant constants)and expressed in terms of the normalized effective field $h_\kappa \equiv \tilde{H}_\kappa / J$

$$E = \alpha J_K \frac{p}{N_1} M - J_{af} m_1 m_2 - \sum_{\kappa=1,2} [\alpha h_\kappa(p) erf(h_\kappa(p)) + (1-\alpha) h_\kappa(0) erf(h_\kappa(0))]$$
$$- J\sqrt{\frac{2}{\pi}} \sum_{\kappa=1,2} [\alpha exp(-h_\kappa^2(p)/2) + (1-\alpha) exp(-h_\kappa^2(0)/2)] - \frac{1}{N}|H + J_K M| \qquad (8)$$

The $T = 0$ selfconsistency equations follow as

$$m_\kappa = -\frac{N_1}{N} erf(\frac{J_{af} m_{\bar{\kappa}} - J_K\ p/N_1 - H}{\sqrt{2q_\kappa} J}) - \frac{N - N_1}{N} erf(\frac{J_{af} m_{\bar{\kappa}} - H}{\sqrt{2q_\kappa} J}), \quad \text{with} \quad \kappa = 1, 2 \quad \text{and} \quad q_\kappa = 1 \qquad (9)$$

where $\bar{\kappa}$ indicates the adjoint of sublattice κ. We evaluate the energy $E = F(T = 0)$ for the multi-valued solutions of the selfconsistent equations in order to select their physical branches. The answer is nontrivial from the start, since the competition between ferromagnetic s-d coupling and antiferromagnetic interaction - and in addition the destructive action of the frustrated part, which behaves differently with respect to ferromagnetic or antiferromagnetic ordering once a field is present - may lead to either one of $p = 0$ or $p = 1$.

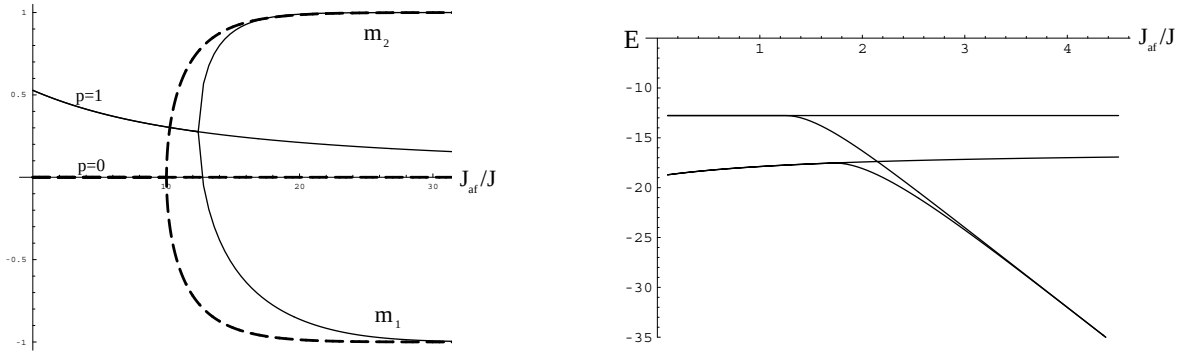

FIG. 2. Fig a: Sublattice magnetizations (set of possible solutions of the selfconsistency equations at zero temperature), shown as a function of the antiferromagnetic coupling J_{af} and classified by hole polarization $p = 1$ or by $p = 0$ (dashed). For large enough J_{af} the sublattice magnetizations start to differ allowing an antiferromagnetic phase ($p = 0$) or an (anti)ferrimagnetic phase ($p = 0$), which approaches saturated staggered order in the large J_{af} limit. Fig b: Transitions between the two forks occur as the ground state energies show.

The $p = 1$ class of solutions bifurcate at higher J_{af} than the $p = 0$ class. This is because the effective non-staggered field induced by the hole polarization is opposed to the antiferromagnetic order. In addition the frustrated part of the interaction also competes with antiferromagnetism and is responsible for the breakdown of different sublattice magnetization (at the bifurcation points). There is also a competition between ferromagnetic and spin glass order, but the source of the effective polaron field is spatially separated and survives in a $p = 1$ solution. Note that we did not display the spin glass order parameters. Working at $T = 0$ they assume their maximum value 1 everywhere, thus

by definition one calls the $p = 0$ type solution with equal sublattice magnetizations (small J_{af}-regime) a spin glass phase, the $p = 1$ type solution (under the same conditions) a dirty ferromagnet. In the large J_{af}-regime the split up sublattice magnetizations are more stable; their $p = 0$ type solution would be a dirty antiferromagnet, while $p = 1$ is a dirty (anti)ferrimagnet.
A special point arises when one of the sublattice magnetizations changes sign and becomes exactly zero. Thus one sublattice becomes nonmagnetic, while the other is ferromagnetic with doubled lattice constant.

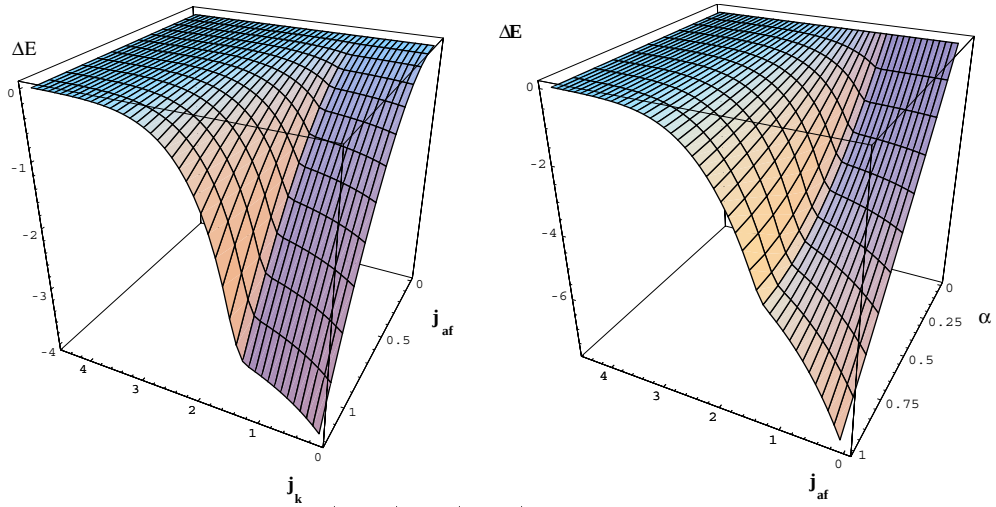

FIG. 3. Difference of ground state energies $E(p = 1) - E(p = 0)$ for hole polarizations $p = 1$ and $p = 0$, shown as a function of $j_{af} \equiv J_{af}/J$, $j_k \equiv J_K/(N_1 J)$, and polaron partition size $\alpha \equiv \frac{N_1}{N}$.

The ground state energy of the hole-polarized $p = 1$-state is always lower than the unpolarized state, no matter whether the sublattice magnetizations are equal or not. Fig.3 shows that for the whole range of exchange couplings and also under arbitrary variation of the polaron size (relative to the entire magnetic barrier) the above statement holds even near the onset of a nonvanishing antiferromagnetic order parameter. Despite the shift of this transition to higher antiferromagnetic coupling in the $p = 1$-case, the lowering of the ground state energy by Δm is not enough to descend below the $p = 1$-energy. As evaluated below the effects of replica symmetry breaking amount to a shift of the transition to a smaller $J^c_{af_{RSB}}$ by roughly the factor $4/5$.
A continuous transition driven by an increasing antiferromagnetic coupling J_{af} into a ferrimagnetic state occurs. The sublattice magnetization m_2 decreases and as the J_{af} grows eventually changes sign.
Due to the model definition the observed $T = 0$ transition is free of quantum-dynamical effects. The classical critical behaviour of the antiferromagnetic order parameter is given by

$$\Delta m \equiv m_1 - m_2 \sim (J_{af} - J^c_{af})^{\frac{1}{2}}, \qquad J_{af} > J^c_{af}. \tag{10}$$

The dependence on the polaron size measured by the number of spins N_1 relative to the total number N is rather weak for smaller couplings j_k, but begins to show a shift and deformation at larger coupling. This appears reasonable, since j_k is opposed to antiferromagnetic order, which is the source of the hole polarization breakdown. Returning to full hole polarization at much higher antiferromagnetic couplings however appears surprising.

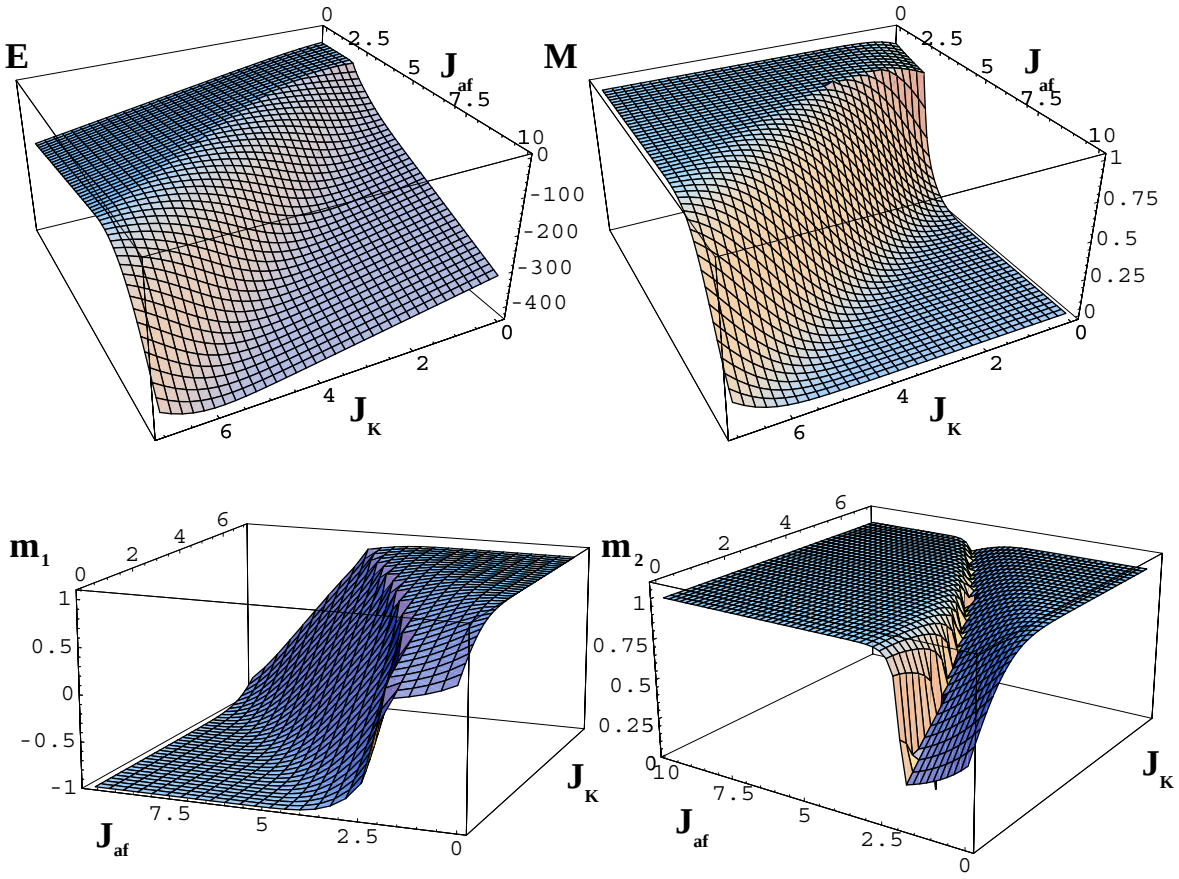

FIG. 4. Energy E, polaron magnetization M, and sublattice magnetizations m_1, m_2 as a function of magnetic field H and of the antiferromagnetic interaction J_{af} are shown for $J = 10$, $N = 2N_1 = 50$ at $T = 0$

Figure 4 shows the $T = 0$ (stable) solutions for polaron magnetization M and sublattice magnetizations m_1, m_2 in a wide range of the J_K- and J_{af}-interactions. The competing effect between ferromagnetic polaron order and transition to antiferromagnetic order of the whole magnetic layer is displayed for polarons filling half the space of the layer, ie $N_1/N = \frac{1}{2}$. The $\alpha = \frac{N_1}{N}$-dependence is weak and the result represents well enough the general case. The selfconsistent equations show that there exists however too a dependence on the polaron spin coordination number N_1 (keeping J_K fixed), which is not expressed in terms of α. This will play an important role for the thermal behaviour of the model.

IV. DIFFERENT SCENARIOS OF THERMAL PHASE TRANSITIONS

In the multi-parameter space various different sequences of phase transitions occur as a function of temperature. While the hole polarized state at $T = 0$ was seen to be stable for all parameters, for certain parameters nonmonotonuous thermal behaviour occurs in $p(T)$ and in related quantities such as polaron magnetization.

A. Domain of sudden hole depolarization and reentrance

The expected thermal decay of polarization at a temperature related to the ferromagnetic interaction $J_K (>> J_{h-h})$ and to the polaron partition, given by the ratio $\alpha = N_1/N$, is preceded by a less expected breakdown in a low temperature interval. We are going to provide detailed solutions for this case in Figures 5,6,7 below.

1. Discontinuous breakdown and restoration of hole polarization; transitions between four magnetic phases with $T_{polaron} > T_c^{ferri} > T_c^{antiferro} > T_c^{ferri2}$

In Figure 5 the hole polarization is plotted together with the sublattice magnetizations and with the spin glass order parameters. One observes a discontinuous drop to zero of the polarization and hence a destruction of the magnetic polaron in a temperature range between $T \approx 1$ and $T \approx 12$. The discontinuous restoration of p induces also discontinuous changes of magnetizations and SG order parameters. In the $p = 0$ interval an antiferromagnetic phase with almost saturated order exists. Complete saturation at $T = 0$ cannot be reached, since as the $T = 0$ results had already shown the $p = 1$ solution is always stable at $T = 0$ and renders $m_1 + m_2$ finite. The analogous sublattice asymmetry of the EA order parameters q_1, q_2 exists but is invisibly small in Fig. 5. In turn the sublattice splitting beyond p-restoration at higher temperatures is relatively large. The magnetization splitting is of course reflected in $m_1 + m_2$. The phase between p-restoration and the breakdown of the antiferromagnetic order parameter at $T \approx 29$, which is related to the antiferromagnetic coupling $J_{af} = 30$ is called ferrimagnetic. Close to the latter transition it has an almost ferromagnetic character, while on the low temperature side it is almost antiferromagnetic. In between it crosses over smoothly between these two opposite limits and on this way one sublattice magnetization eventually becomes zero and changes sign.

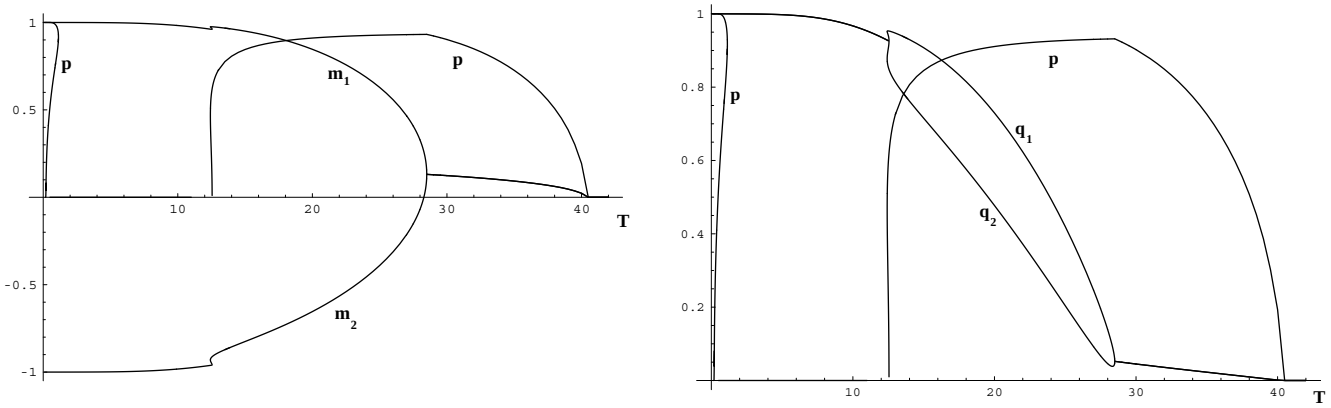

FIG. 5. A sequence of phase transitions is shown for the parameter choice of $J = 8, J_K = 12, J_{af} = 30$: below $T_p \approx 40$ the ferromagnetic polaron is formed in a pseudo phase transition, followed by a continuous antiferromagnetic phase transition into a ferrimagnetic phase with sublattice-asymmetric spin glass order parameters $q_1 \neq q_2$; at still lower T one sublattice magnetization changes sign slowly and, before reaching perfect antiferromagnetic order, the hole polarization undergoes a sharp drop to zero. Before the $T = 0$ limit is reached the reentrant discontinuous phase transition into the hole polarized state takes place.

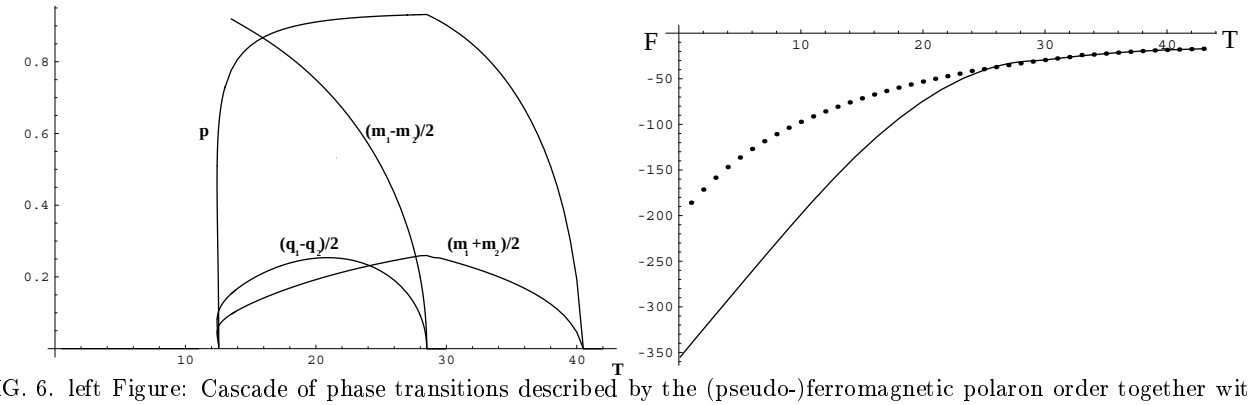

FIG. 6. left Figure: Cascade of phase transitions described by the (pseudo-)ferromagnetic polaron order together with the hole polarization p and with antiferromagnetic order parameters $m_2 - m_1$ and $q_2 - q_1$; right Figure: free energies for the stable hole-polarized and for the $p = 0$ solution (dotted curve)

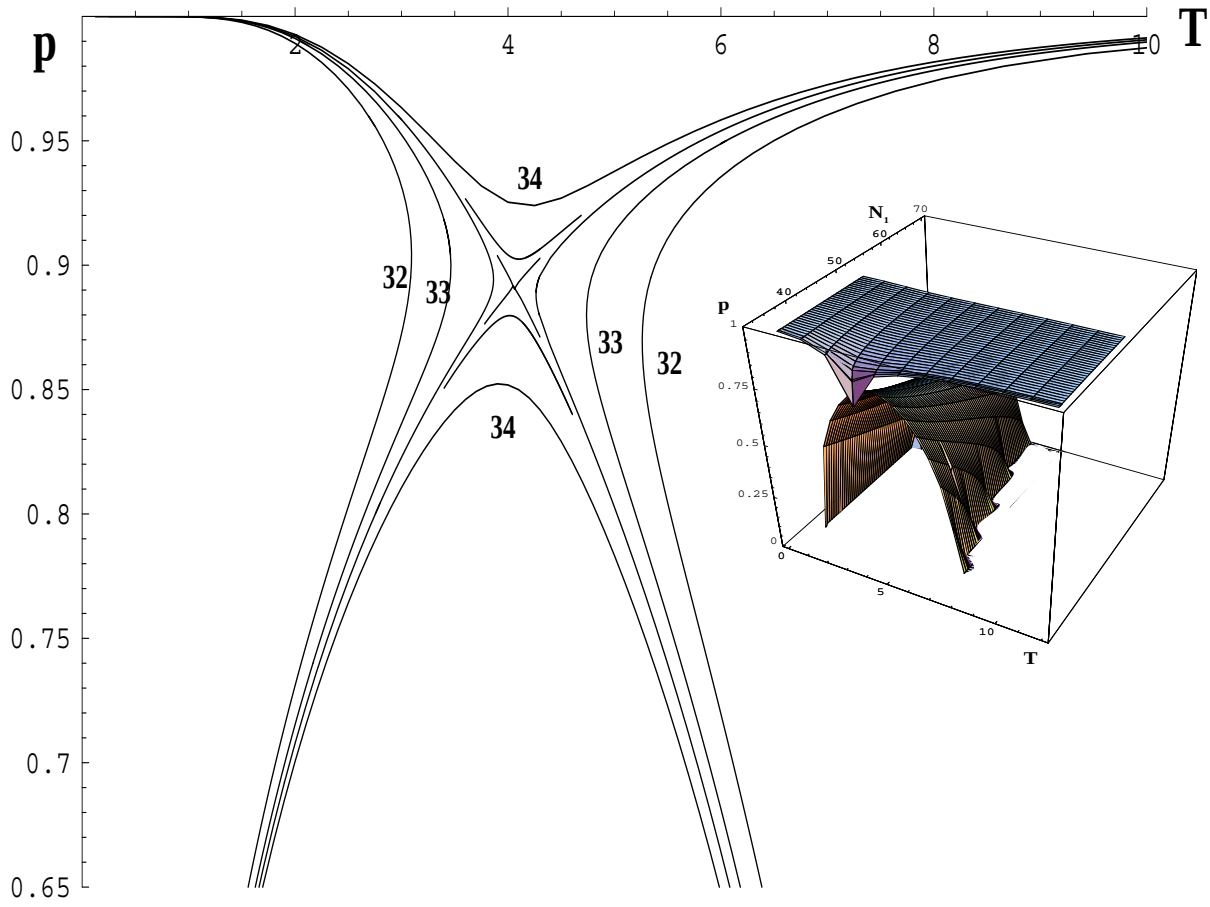

FIG. 7. Main figure: Cross sections through the surface of selfconsistent solutions for hole polarization p at $J_K = 12, J = 8, J_{af} = 30$, displayed as a function of temperature for chosen numbers N_1 of associated polaron spins. The Figure shows curves for $N_1 = 32, 33, and 34$ and also uses noninteger values 33.5, 33.6 to approach the point of intersection at $N_1 = 33.555$. The higher value of the double-valued polarization solution forms the stable branch. The totally depolarized interval appears below $N_1 = N_c \approx 33.555$; for this parameter the otherwise disconnected surfaces intersect. The inserted figure shows two surfaces of solutions for the hole polarization as obtained for polarons with spin number $N_1 > N_c = 33.555$. The onset of hole depolarization for $N < N_c$ is seen in front.

We have analyzed the parameter region and in particular the N_1-dependence of the polaron breakdown regime. As described before the almost antiferromagnetic order is responsible for the breakdown. With increasing spin glass interaction J the p-depleted regime is reduced, since J competes with J_{af} and tends to depress antiferromagnetic order. In the examples of Figures 5-7 the ratio $J_{af}/J = 15/4$ favours strongly low temperature antiferromagnetic order and, as shown before, a reentrant transition into the $p = 1$ state at $T = 0$ must occur despite the almost perfect antiferromagnetic order. The α-dependence of the breakdown-regime on the polaron partition within the magnetic layer is rather weak and insignificant. The N_1-dependence describing the coordination number of polaron spins with each exciton is however strong as Figure 7 shows. For the range of N_1 Villain-pseudospins considered here, the behaviour of a $CdMnTe$-layer is three-dimensional bulk-like (no matter how large α).

B. Monotonuous thermal decay of hole-polarization

Still several different sequences of magnetic phase transitions occur when the peculiar feature of p-depression and p-restoration in a low temperature interval is absent. The hole polarization then decreases as the temperature increases, but nonanalytical behaviour still emerges as a secondary effect of transitions driven by the antiferromagnetic interaction for example.

1. Fully hole polarized phase with intermediate ferrimagnetic phase in the regime $T_{polaron} > T_c^{antiferro} > T_{SG}$

In Figure 8 the reentrance in a dirty ferromagnetic phase appears. The parameter choice is known to be problematic w.r.t. spin glass reentrance in the absence of an external field and requires replica symmetry breaking. An intermediate ferrimagnetic phase with strong antiferromagnetic character occurs in between. The onset of sublattice asymmetry can be seen as an antiferromagnetic transition as well. The low temperature phase can be predominantly a spin glass phase in a polaron field caused by the s-d interaction.

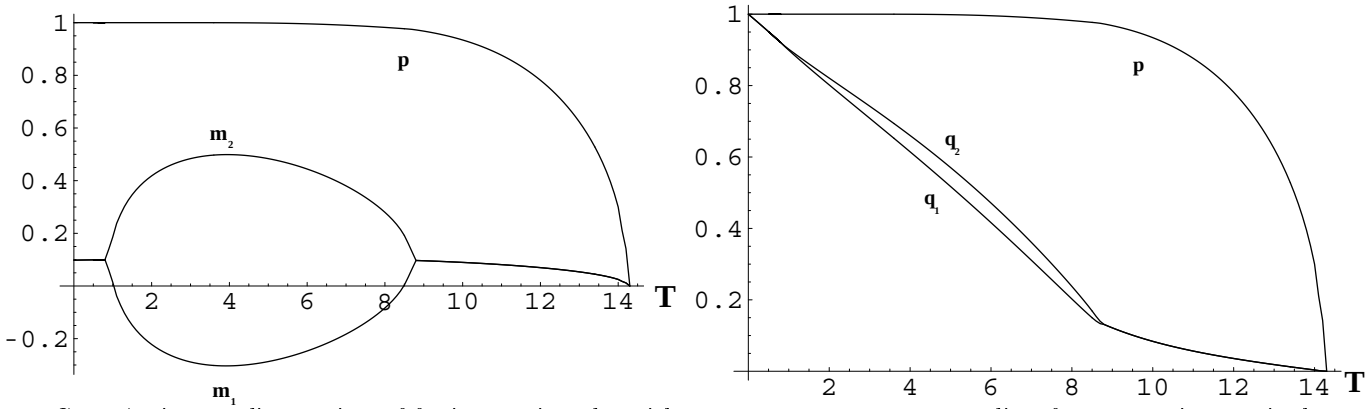

FIG. 8. An intermediate regime of ferrimagnetic order with reentrant transitions into a dirty ferromagnetic state is shown for $J_K = 2, J = 8, J_{af} = 10$

2. Low temperature ferrimagnetic (almost-antiferromagnetic) phase induced by hole polarization: sequence of critical points $T_c^{antiferro} > T_c^{ferri}$

Figure 9 represents the case where the antiferromagnetic transition occurs first, followed at lower temperatures by the polaron formation. The latter inevitably leads to the sublattice splitting of the EA order parameters and of $-m_1$ and m_2 as well. In accordance with the $T = 0$ result the sublattice magnetizations, in contrast to q_1, q_2, cannot fully saturate because of the polaron field. The critical behaviour of $q_1 - q_2$ and of $m_1 + m_2$ at the polaron transition agrees. This is clearly suggested by Figure 11 and confirmed in the analytical calculation. The standard linear behaviour of SG order parameters is absent. Instead of $\beta = 1$, one observes $q_1 - q_2 \sim \tau^\beta$ with $\beta = \frac{1}{2}$.

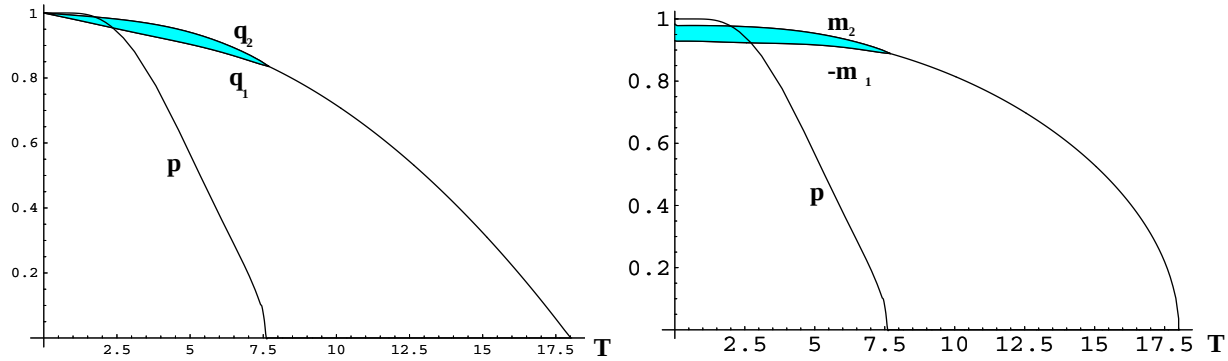

FIG. 9. Sublattice anisotropy of q_1, q_2 (left) and $-m_1, m_2$ (right) in the regime of monotonuous hole polarization with $J_K = 5, J_{af} = 18, \alpha = .5$.

The onset of a finite polaron exchange field at T_p can be estimated analytically from our selfconsistent equations, finding

$$T_p \sim T_p^0 \; exp(-J_{af}/T_p^0) \quad \text{with} \quad T_p^0 = J_K/\sqrt{2N_1} \tag{11}$$

One may also consider the case of s-d couplings large in comparison to the competing interactions so that the polaron magnetization sets in at the highest temperature. Of course the present description is still on mean field level - an exact treatment of the s-d coupling has not yet been achieved - and, taking each polaron as a small independent system of a finite number of particles the picture of a true phase transition is an artifact of the mean field Ansatz. However, an arbitrarily small ferromagnetic hole-hole interaction and the infinite-range J- and J_{af}-interactions correlate the polarons and the fluctuations can be assumed to be less dangerous for the polaron transition. For comparison with experiments in small fields the mean field approximation becomes very useful and, theoretically, one can also imagine the smearing of the transition in a magnetic field (see Figures 15 and 16 below) as an analogy to finite size effects in zero field.

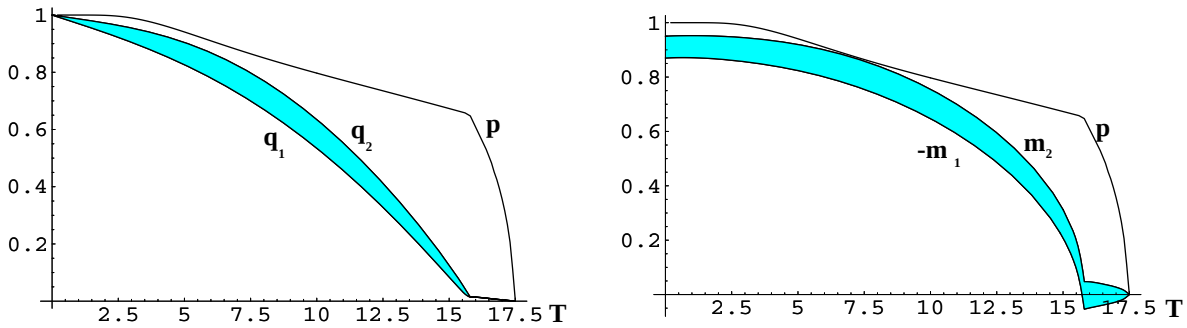

FIG. 10. Regime of ferromagnetic polaron transition followed by antiferromagnetic transition at slightly lower temperature with $J_K = 5, J_{af} = 16, \alpha = .5$. The Figure displays the sublattice anisotropy (shaded region) of spin glass order parameters (left) and of $-m_1, m_2$ (right) together with the hole polarization p.

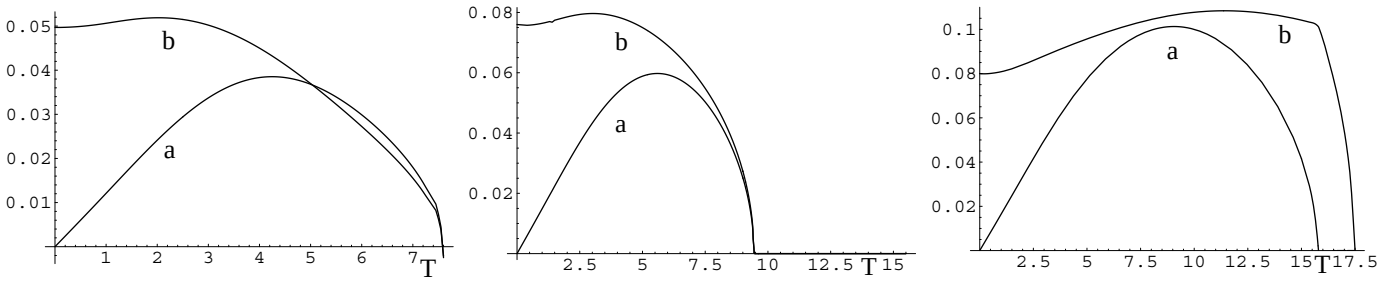

FIG. 11. Difference of sublattice EA order parameters $q_2 - q_1$ (curve a) and sum of sublattice magnetizations $(m_1 + m_2)/2$ (curve b) for $J_K = 5, J_{af} = 18$ (left), $J_K = 4, J_{af} = 15$ (middle), and $J_K = 5, J_{af} = 16$ (right).

Figure 11 reconsiders the parameter sets of the Figures above and compares $q_2 - q_1$ with $m_1 + m_2$: for $T_c^{antiferro} > T_{polaron}$ and at the ferrimagnetic transition the order parameters behave like $(T_c^{ferri} - T)^{\frac{1}{2}}$. In the low temperature limit $m_1 + m_2$ approach the numerically determined finite limit, which represents the incomplete antiferromagnetic order caused by the $p(T = 0) = 1$ hole polarized state. In a low temperature expansion, the linear behaviour of the sublattice asymmetry of the spin glass order parameter is confirmed by

$$q_2 - q_1 = 2\alpha \frac{T}{J} \sqrt{\frac{2}{\pi}} exp(-\frac{J_{af}^2 + h_{exch}^2}{2J^2}) sinh(\frac{J_{af} h_{exch}}{J^2}), \qquad \text{with} \qquad h_{exch} \equiv J_K \, \frac{p}{2N_1}. \tag{12}$$

Of course the low T limit undergoes corrections from replica symmetry breaking.

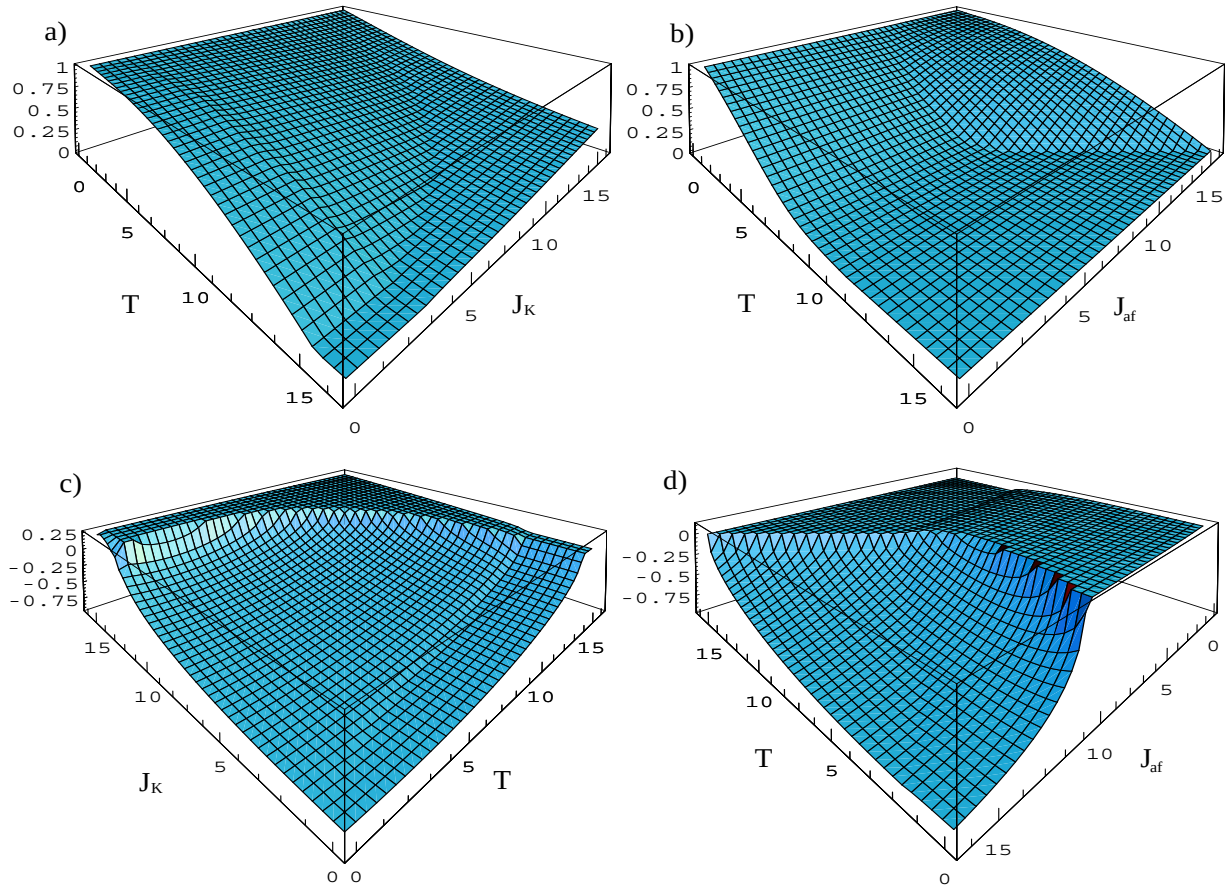

FIG. 12. Spin glass order parameter a),b) and sublattice magnetization c),d) for sublattice 1 as function of the temperature, J_K and J_{af}. The parameters are chosen as $\alpha = 0.5, J = 8K, J_{af} = 15K$(for a and c) and $J_K = 2K$ (for b and d).

4. Spin glass limit and high polaron temperature

To make contact with the parameter regime explored in Ref. 5 we add the evaluation shown in Figure13 which elaborates the characteristic feature of a maximum in the magnetization, for which the frustrated interaction J is responsible. The s-d coupling assumed the high value $J_K = 15$, which leads to a high polaron temperature $T_p \approx 105$ in accordance with the estimation rule of Ref. 5. High T_p implies a large exchange field, which smears strongly the spin glass transition.
Since the present work does not focus on quantitative comparison we do not attempt here to model the experimental curve for 33% manganese by replacing the assumption of small antiferromagnetic clusters by a corresponding antiferromagnetic interaction.

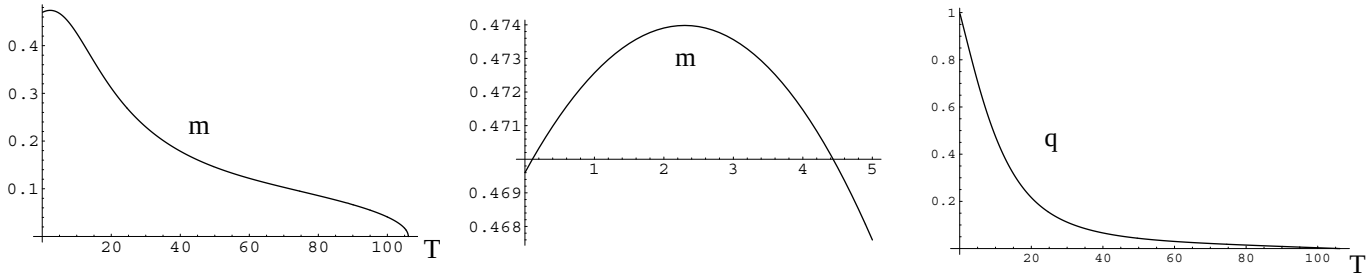

FIG. 13. Magnetization (left), its low temperature maximum (middle), and the spin glass order parameter (right), shown for $J_K = 15, J = 8, N_1 = 50, \alpha = .5$ and vanishing antiferromagnetic interaction. The spin glass order parameter shows the typical smearing effect in the large exchange field of the polaron with high temperature $T_p \approx 105$.

Further calculations with finite antiferromagnetic couplings show that the maximum becomes less pronounced since increasing J_{af} depresses $m(T=0)$ in the spin glass phase as our $T=0$ calculations above show. The position of the maximum remains however almost unshifted.

V. BEHAVIOUR IN A MAGNETIC FIELD

The application of a homogeneous field does not destroy the antiferromagnetic phase transition discussed above, but affects the competition between the effective interactions. The ferromanetic alignment of all polaron spins is supported by the field. It is thus particularly interesting to study the polaron restoration in the breakdown regime of Fig.5. The following solutions are obtained at $T=0$

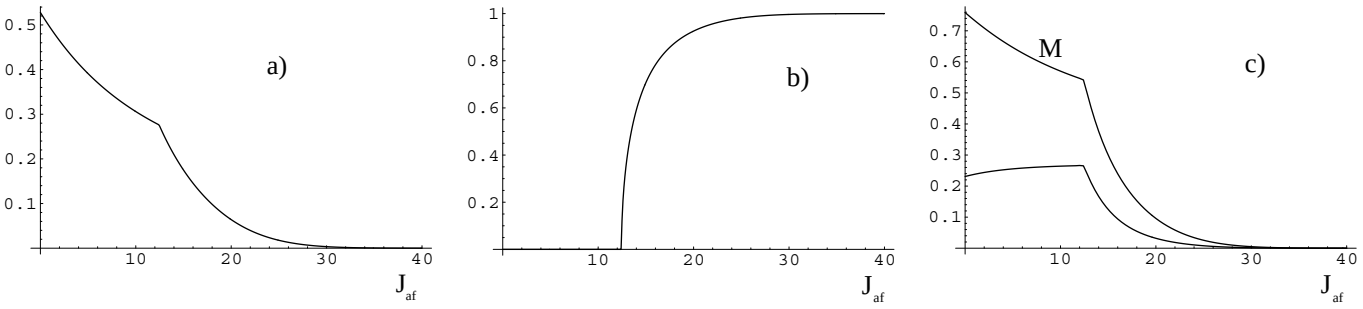

FIG. 14. The glassy ferromagnetic–ferrimagnetic transition driven by the growing antiferromagnetic interaction at $T=0$ and in a homogeneous external magnetic field H is displayed for $0 < J_{af}/J < 3.5$. Part a) shows the sum of sublattice magnetization, b) the antiferromagnetic order parameter and c) the polaron magnetization M together with $M-(m_1+m_2)/2$ (curve below).

The discontinuity in the zero field transition must be reconsidered in the light of the Falicov-Hui-Berker conclucions[12,13], once the infinite-range simplification is given up. These authors showed that disorder in many cases turns a discontinuous transition of the mean field theory into a continuous one, if fluctuations are taken into account in realistic dimensions. Whether the partially frustrated interaction can change this general conclusion can not yet be answered and we hope to come back to this question in the context of renormalization of the present phase transitions.

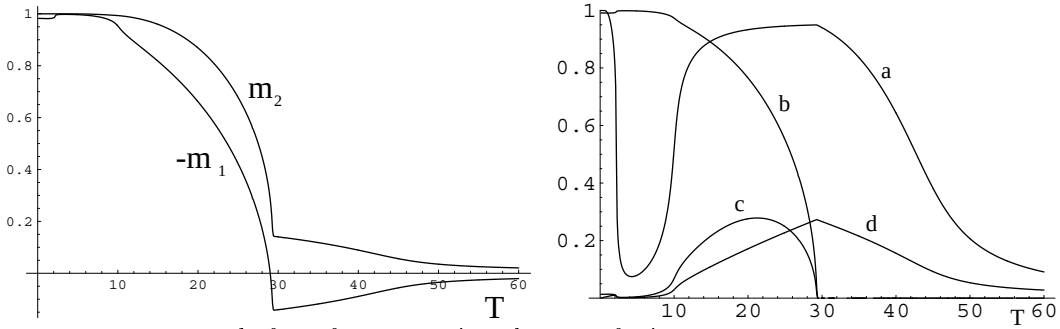

FIG. 15. Phase transition cascade from ferromagnetic polaron to ferrimagnet with strong anisotropic spin glass overlap via hole depolarization with almost antiferromagnetic order to polaron restoration and antiferromagnetic order at lowest temperatures. The Figure shows sublattice magnetizations $-m_1$ and m_2 (left part of Figure) and hole polarization p (a), order parameters $(m_1+m_2)/2$ (d) for the smeared ferromagnetic transition in small magnetic field $\mu H/J_K \approx \frac{1}{8}$ and $(m_2-m_1)/2$ (b), q_1-q_2 (c) (in the right part) for the unaltered sharp antiferromagnetic transition at $T_{af} \approx J_{af} = 30$.

As the magnetic field increases the ferromagnetic- and (not shown here) spin glass transitions become smeared while the antiferro-type order parameters m_1-m_2 or q_1-q_2 signalling the onset of ferrimagnetic order remain sharp. The hole-polarization is restored fast by an increasingly large magnetic field as Figure 16 shows and the secondary features in the polaron magnetization and in the sublattice anisotropy of the spin glass order parameter are washed out too.

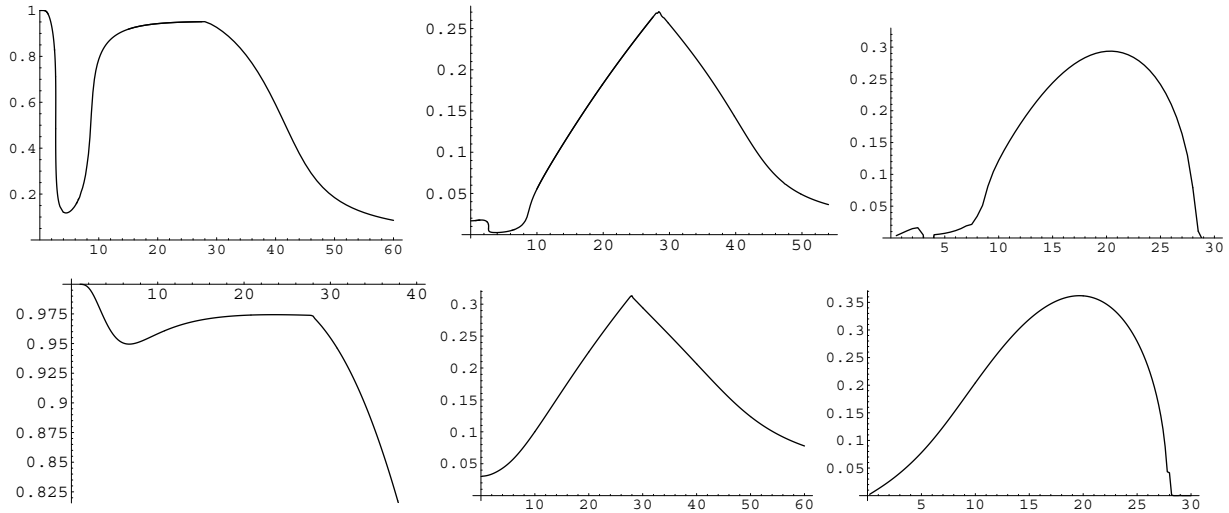

FIG. 16. Polaron restoration in a magnetic field shown in p, M, and sublattice asymmetry of $q_1 - q_2$, for magnetic fields $H = 1$ (upper row from left) and $H = 3$ (second row from left) with coupling constants $J_K = 12, J = 8, J_{af} = 30, N_1 = 16 = \frac{2}{3}N$.

VI. REGIONS OF PHASE DIAGRAM AFFECTED BY REPLICA SYMMETRY BREAKING: DE ALMEIDA THOULESS SURFACE

In order to analyze the stability of the replica-symmetric (RS) solution (5-7) let us consider the small deviation from the RS-form of matrix Q^{ab}

$$Q^{ab} = q + \phi^{ab}, \qquad Q_1^{ab} = q_1 + \phi_1^{ab}, \qquad Q_2^{ab} = q_2 + \phi_2^{ab}. \tag{13}$$

As follows from (1), the fluctuations inside and outside magnetic polaron are completely decoupled. This means that one should consider the stability of RS solution either inside or outside the MP. Unlike the conventional de Almeida Thouless analysis, there exist two magnetic fields in the magnetic polaron problem. One field is related to the $s - d$ coupling of the hole-spin with its environment, providing an effective internal magnetic field. Another one represents the usual external magnetic field. Taking both into account we discuss the AT-surface (temperature vs two magnetic fields) which determines the stability region of the RS-solution. Since the coupling of the magnetic polaron (MP) with environment is chosen positive (ferromagnetic coupling), the AT surface corresponding to the solution outside the MP is related to effectively higher magnetic fields $H_{eff} = H + h_{exch} > H$ where $h_{exch} = J_K p/(2N_1)$ and thus lies above the AT surface calculated for the region inside MP. Therefore we consider only the AT surface outside magnetic polaron.

According to the standard procedure the expansion of the free energy up to second order in $\vec{\phi}^T = (\phi \quad \phi_1 \quad \phi_2)$ is given by:

$$\beta f[\vec{q}, \vec{\phi}] = \beta f_{SP}[q] + \frac{(\beta J)^2}{8n} \sum_{ab,cd} \vec{\phi}^T G_{ab,cd} \vec{\phi}. \tag{14}$$

where $G_{ab,cd}$ reads as follows

$$G_{ab,cd} = \begin{pmatrix} \delta_{ab,cd} - (\beta J)^2 \Delta(S_1 + S_2)^4 & -i(\beta J)^2 \Delta(S_1)^4 & -i(\beta J)^2 \Delta(S_2)^4 \\ -i(\beta J)^2 \Delta(S_1)^4 & \delta_{ab,cd} + (\beta J)^2 \Delta(S_1)^4 & 0 \\ -i(\beta J)^2 \Delta(S_2)^4 & 0 & \delta_{ab,cd} + (\beta J)^2 \Delta(S_2)^4 \end{pmatrix}. \tag{15}$$

We denote $\Delta(\sigma)^4 = < \sigma^a \sigma^b \sigma^c \sigma^d > - < \sigma^a \sigma^b >< \sigma^c \sigma^d >$. In order to find the condition for instability of RS solution it is sufficient to take the eigenfunction corresponding to instability of FM SK model[9]. The equation for the eigenvalue λ has the form

$$\begin{vmatrix} g - \lambda & g_1 & g_2 \\ g_1 & g_{11} - \lambda & 0 \\ g_2 & 0 & g_{22} - \lambda \end{vmatrix} = 0 \tag{16}$$

where the matrix elements g are given by

$$g_{1,2} = -i(\beta J)^2 \int_z^G \cosh^{-4}\left(\beta\tilde{H}_{1,2}\right), \qquad g_{11,22} = 1 + (\beta J)^2 \int_z^G \cosh^{-4}\left(\beta\tilde{H}_{1,2}\right),$$

$$g = 1 - (\beta J)^2 \int_z^G \left(\cosh^{-4}\left(\beta\tilde{H}_1\right) + \cosh^{-4}\left(\beta\tilde{H}_2\right)\right). \tag{17}$$

Substituting these matrix elements into expression (16), the new equation for the AT-surface is obtained. Thus, the replica symmetric solution outside the magnetic polaron is stable when

$$\left(\frac{T}{J}\right)^4 > \int_z^G \cosh^{-4}\left(\beta\tilde{H}_1\right) \int_z^G \cosh^{-4}\left(\beta\tilde{H}_2\right). \tag{18}$$

The result of numerical solution of equation (18) together with (5-7) is presented in Fig.17

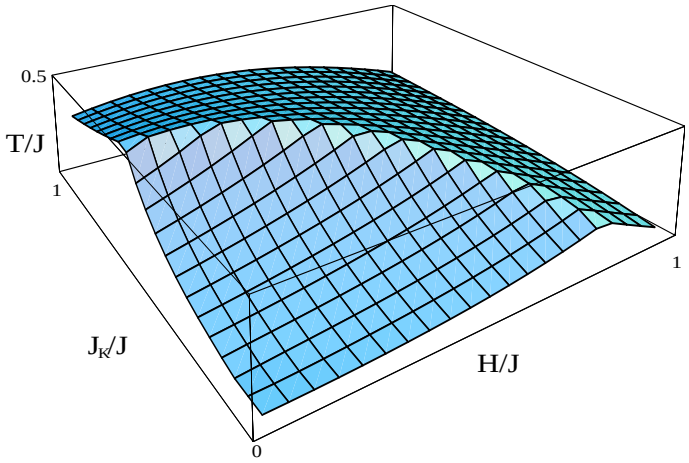

FIG. 17. AT-surface for magnetic polaron problem ($J_{af}/J = 1.9$, $\alpha = 0.5$)

The behaviour of AT-lines (the projections to $T - H$ and $T - h_{exch}$ planes) is shown by Fig18-19. As it was pointed out in Ref. 9 for two-sublattices SK-antiferromagnets, the AT line is a nonmonotonuous function of external (or internal) magnetic field with a kink at $H^0_{eff} \sim T_N(0)$. At fields $H_{eff} \gg J_{af}$ the freezing temperature T_f decreases exponentially with increasing magnetic field $T_f(H) \sim J\exp\left(-(H_{eff} - J_{af})^2/(2J^2)\right)$. We note that the unusual behaviour of the AT-line exists only when $J_{af}/J > 1$. Nevertheless, even in this case two possibility can be considered. In both cases the staggered magnetization is not equal to 0 above and below the AT-line providing the existence of nonergodic AF state. The criterion of the AF-instability reads as follows

$$\left[1 - J_{af}\left(\alpha\chi_{\bar{H}+h_{exch}} + (1-\alpha)\chi_{\bar{H}}\right)\right]\left[1 + J\left(\alpha\phi_{\bar{H}+h_{exch}} + (1-\alpha)\phi_{\bar{H}}\right)\right] +$$

$$+J_{af}J\left(\alpha\psi_{\bar{H}+h_{exch}} + (1-\alpha)\psi\tilde{H}\right)\left(\alpha\varphi_{\bar{H}+h_{exch}} + (1-\alpha)\varphi_{\bar{H}}\right) = 0$$

where

$$\chi_{\bar{H}} = \beta\int_z^G \cosh^{-2}(\beta\tilde{H}), \qquad \phi_{\bar{H}} = \beta\int_z^G \frac{z}{\sqrt{q}}\tanh(\beta\tilde{H})\cosh^{-2}(\beta\tilde{H}),$$

$$\psi_{\bar{H}} = \beta\int_z^G \tanh(\beta\tilde{H})\cosh^{-2}(\beta\tilde{H}), \qquad \varphi_{\bar{H}} = \beta\int_z^G \frac{z}{\sqrt{q}}\cosh^{-2}(\beta\tilde{H}).$$

with $\tilde{H} = Jz\sqrt{q} - J_{af}m + H$.
Nevertheless, in the case shown in Fig.18a, and corresponding to $J_{af} \sim J$, the nonergodic AF state ends up at finite

temperature at zero field whereas when $J_{af} \gg J$ (Fig.19a), the nonergodic AFM exists at $T = 0$. Nonmonotonuous behaviour of T_f occurs due to the interplay between magnetic field, spin glass and antiferromagnetic states. Generally speaking, this competition results in suppression of both, AF- and SG-state, by an external magnetic field. Nevertheless, since suppression of one order parameter is favorable for another one, there exist a region of magnetic fields, where suppression of the AF-phase facilitates the appearance of the spin glass.

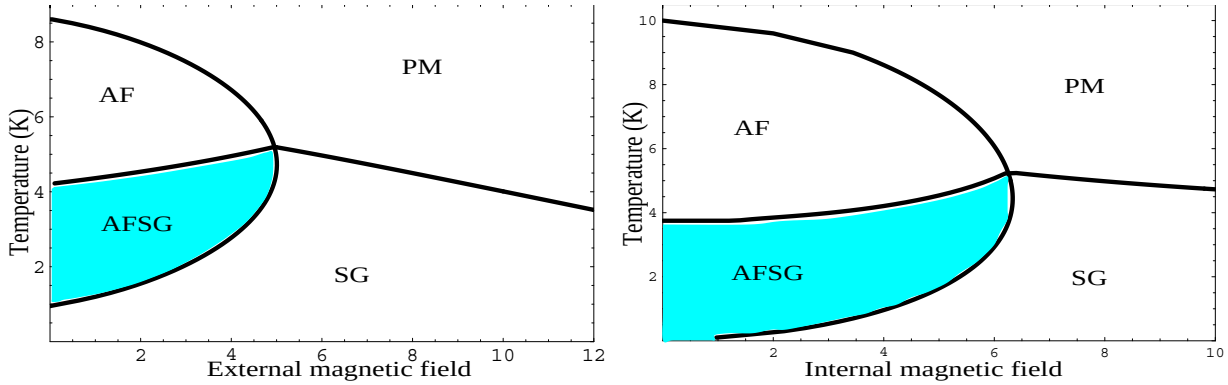

FIG. 18. Nonmonotonuous AT-line for magnetic polaron for glassy antoferromagnet, (a)temperature vs external magnetic field $J_K = 4$, (b)temparature vs J_K, $H = 0$, ($J = 8$,$J_{af} = 10$, $\alpha = 0.5$)

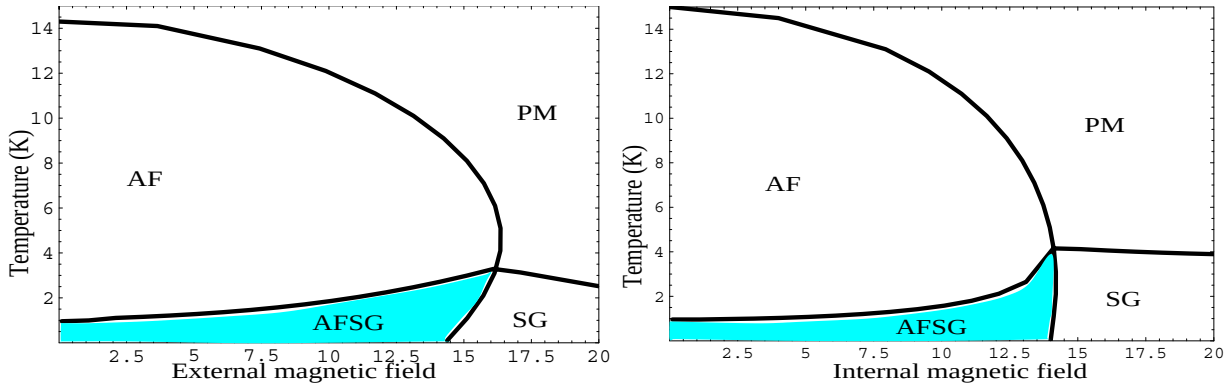

FIG. 19. Nonmonotonuous AT-line for magnetic polaron for the glassy antiferromagnet, (a)AT-temperature vs external magnetic field $J_K = 4$, (b)temperature vs J_K, $H = 0$, ($J = 8$,$J_{af} = 15$, $\alpha = 0.5$)

APPENDIX A

The free energy for 1-step RSB is given by (note that only in this appendix we use capital Letters for all magnetizations in order to avoid confusion with the Parisi parameter m of 1-step RSB)

$$\beta f = \frac{N_1 N_p}{2N_S} J_K \beta \left(\upsilon^2 - \xi^2 - \left(\frac{p}{2N_1} \right)^2 \right) - \frac{N_p}{2N_S} \log \left(2 \cosh \left(\beta \left[H + J_K (\upsilon - \frac{p}{2N_1}) \right] \right) \right) - \frac{\beta J_{af}}{2} \left(2M^2 - \frac{1}{2} M_1^2 - \frac{1}{2} M_2^2 \right) -$$

$$- \frac{(\beta J)^2}{4} \left(2(1 + m q_0^2 + (1-m) q_1^2 - 2q_1) - \frac{1}{2}(1 + m q_{10}^2 + (1-m) q_{11}^2 - 2q_{11}) - \frac{1}{2}(1 + m q_{20}^2 + (1-m) q_{21}^2 - 2q_{21}) \right)$$

$$- \frac{N_1 N_p}{2mN_S} \int_z^G \left(\log \left(\int_y^G \left[2 \cosh \left(\beta (Jz\sqrt{2q_0 - q_{10}} + Jy\sqrt{2q_1 - q_{11} - 2q_0 + q_{10}} + H + J_K(\upsilon - \xi) - J_{af}(2M - M_1) \right) \right]^m \right) \right) +$$

$$+\log\left(\int_y^G\left[2\cosh\left(\beta(Jz\sqrt{2q_0-q_{20}}+Jy\sqrt{2q_1-q_{21}-2q_0+q_{20}}+H+J_K(\upsilon-\xi)-J_{af}(2M-M_2)\right)\right]^m\right)\right)\Bigg)$$

$$-\frac{N_S-N_1N_p}{2mN_S}\int_z^G\left(\log\left(\int_y^G\left[2\cosh\left(\beta(Jz\sqrt{2q_0-q_{10}}+Jy\sqrt{2q_1-q_{11}-2q_0+q_{10}}+H-J_{af}(2M-M_1)\right)\right]^m\right)\right)+$$

$$+\log\left(\int_y^G\left[2\cosh\left(\beta(Jz\sqrt{2q_0-q_{20}}+Jy\sqrt{2q_1-q_{21}-2q_0+q_{20}}+H-J_{af}(2M-M_2)\right)\right]^m\right)\right)\Bigg). \tag{19}$$

Extremizing the free energy with respect to all parameters the new selfconsistent equations are obtained

$$p=\tanh(\beta(H+J_K\xi)),\qquad \upsilon=\xi+\frac{p}{2N_1},\qquad q_0=\frac{1}{2}(q_{10}+q_{20}),\qquad q_1=\frac{1}{2}(q_{11}+q_{21}),\qquad M=\frac{1}{2}(M_1+M_2). \tag{20}$$

$$\xi=\frac{1}{2}\int_z^G\left(\frac{\int_y^G\mathcal{C}_{2|1}^{m-1}\mathcal{D}_{2|1}}{\int_y^G\mathcal{C}_{2|1}^m}+\frac{\int_y^G\mathcal{C}_{2|2}^{m-1}\mathcal{D}_{2|2}}{\int_y^G\mathcal{C}_{2|2}^m}\right),$$

$$M_{1,2}=\alpha\int_z^G\frac{\int_y^G\mathcal{C}_{2|2,1}^{m-1}\mathcal{D}_{2|2,1}}{\int_y^G\mathcal{C}_{2|2,1}^m}+(1-\alpha)\int_z^G\frac{\int_y^G\mathcal{C}_{1|2,1}^{m-1}\mathcal{D}_{1|2,1}}{\int_y^G\mathcal{C}_{1|2,1}^m},$$

$$q_{1,2\,1}=\alpha\int_z^G\frac{\int_y^G\mathcal{C}_{2|2,1}^{m-2}\mathcal{D}_{2|2,1}^2}{\int_y^G\mathcal{C}_{2|2,1}^m}+(1-\alpha)\int_z^G\frac{\int_y^G\mathcal{C}_{1|2,1}^{m-2}\mathcal{D}_{1|2,1}^2}{\int_y^G\mathcal{C}_{1|2,1}^m},\qquad m\neq 1$$

$$q_{1,2\,0}=\alpha\int_z^G\frac{(\int_y^G\mathcal{C}_{2|2,1}^{m-1}\mathcal{D}_{2|2,1})^2}{(\int_y^G\mathcal{C}_{2|2,1}^m)^2}+(1-\alpha)\int_z^G\frac{(\int_y^G\mathcal{C}_{1|2,1}^{m-1}\mathcal{D}_{1|2,1})^2}{(\int_y^G\mathcal{C}_{1|2,1}^m)^2},\qquad m\neq 0 \tag{21}$$

In two limiting cases $m=0$ and $m=1$ the equations (19) coincide with (5-7) for $q_{1,2}=q_{1,2\,1}$ and $q_{1,2}=q_{1,2\,0}$ respectively. The equation for Parisi parameter m is given by

$$\frac{(\beta J)^2}{4}(q_{10}q_{20}-q_{11}q_{21})=\frac{1}{2m^2}\int_z^G\left(\alpha\left[\log(\int_y^G\mathcal{C}_{2|1}^m)+\log(\int_y^G\mathcal{C}_{2|2}^m)\right]+(1-\alpha)\left[\log(\int_y^G\mathcal{C}_{1|1}^m)+\log(\int_y^G\mathcal{C}_{1|2}^m)\right]\right)-$$

$$-\frac{1}{2m}\int_z^G\left(\alpha\left[\frac{\int_y^G\mathcal{C}_{2|1}^m\log\mathcal{C}_{2|1}}{\int_y^G\mathcal{C}_{2|1}^m}+\frac{\int_y^G\mathcal{C}_{2|2}^m\log\mathcal{C}_{2|2}}{\int_y^G\mathcal{C}_{2|2}^m}\right]+(1-\alpha)\left[\frac{\int_y^G\mathcal{C}_{1|1}^m\log\mathcal{C}_{1|1}}{\int_y^G\mathcal{C}_{1|1}^m}+\frac{\int_y^G\mathcal{C}_{1|2}^m\log\mathcal{C}_{1|2}}{\int_y^G\mathcal{C}_{1|2}^m}\right]\right),$$

where the following notations are introduced

$$\mathcal{C}_{1|1,2}=2\cosh(\beta\tilde{H}_{1,2}^{(1)}),\quad \mathcal{C}_{2|1,2}=2\cosh(\beta(\tilde{H}_{1,2}^{(1)}+h_{exch})),\quad \mathcal{D}_{1|1,2}=2\sinh(\beta\tilde{H}_{1,2}^{(1)}),\quad \mathcal{D}_{2|1,2}=2\sinh(\beta(\tilde{H}_{1,2}^{(1)}+h_{exch})),$$

$$\tilde{H}_{1,2}^{(1)}=Jz\sqrt{q_{1,2\,0}}+Jy\sqrt{q_{1,2\,1}-q_{1,2\,0}}-J_{af}m_{1,2}+H.$$

VII. CONCLUSIONS

We analyzed a model which describes layered II-VI semiconductors, where interface-localized exciton holes interact with spins of the magnetic layer, forming thus magnetic polarons. The interplay between antiferromagnetic (AFM), spin glass (SG) and ferromagnetic (FM) order in the magnetic layer is taken into account. The competition between different correlations explains the rich phase diagram of the model. We have shown that the tendency of AFM ordering in the two sublattice Ising-like magnet results in depolarization of the magnetic polaron within a certain range of parameters, which depends e.g. on polaron-size, on the relative strength of the AFM and frustrated interaction. This polarization breakdown occurs in a discontinuous transition (for zero external magnetic field) at temperatures where AFM order is almost reached; its restoration at lowest temperatures also takes place discontinuously. The competition between AFM and SG ordering in the presence of an internal magnetic field, related to the magnetic polaron, also leads to nonmonotonuous behaviour of the Almeida-Thouless line beyond which ergodicity breaking occurs. This antiferromagnetic effect enlarges the validity regime of the replica symmetric solution. We have shown that the existence of locally confined magnetic fields due to magnetic polarons gives rise to an unusual spin glass state with different Edwards-Anderson order parameters for different sublattices. This phase may be called ferrimagnetic spin glass (ferri-SG). The mean-field critical exponents in the vicinity of the ferri-SG transition point are different from those in conventional SG theory. The various magnetic phases and transitions between them are analyzed in the low temperature limit. It is shown that only the spin-polarized solution is stable, providing nevertheless the possibility of a classical (free of quantum-dynamical effects) antiferromagnetic transition at $T = 0$. We have discussed in detail the behaviour of the magnetic polaron in weak external magnetic fields. Although in such fields the magnetic polaron is preformed at high temperatures, the almost total breakdown of the hole polarization is shown to occur due to the antiferromagnetic interaction. We propose to verify the theoretical predictions made in the paper by experiments on $CdTe/Cd_{1-x}Mn_xTe$ for high manganese concentrations.

VIII. ACKNOWLEDGMENTS

This work was supported by the EPSRC (R.O., D.S.), by the Humboldt foundation (M.K.), and by the SFB410 II-VI semiconductors. One of us (R.O.) wishes to thank for hospitality of the Department of Physics of Oxford university extended to him during his stay. M.K. also wishes to express his gratitude to Heiko Feldmann for helpful assistance and we feel indebted to G. Landwehr for suggesting the magnetic field analysis of the CdTe/CdMnTe model.

---

[1] M.B. Weissman, N.E. Israeloff, and G.B. Alers, J.Magn.Magn.Mat.114, 87 (1992)
[2] M.B. Weissman, Rev.Mod.Phys. 65, 829 (1993)
[3] J. Jaroszynski, J. Wrobel, M.Sawicki, E. Kamiska, T.Skoskiewicz, G.Karczewski, T.Wojtowicz, A.Piotrowska, J.Kossut, and T.Dietl, Phys.Rev.Lett.75, 31 (1995)
[4] I.P. Smorchkowa, N. Samarth, J.M. Kikkawa, D.D. Awschalom, Phys.Rev.Lett.78, 3571 (1997)
[5] A. Chudnovskiy, R. Oppermann, B. Rosenow, D. Yakovlev, W. Zehnder, W. Ossau, Phys.Rev.B55, 10519 (1997)
[6] J. Villain, Z.Phys.B33, 31 (1979)
[7] F. Bernardot, C.Rigaux, Phys.Rev.B56, 2328 (1997)
[8] C. Wengel, C.L. Henley, A. Zippelius, Phys.Rev. B53, 6543 (1995)
[9] I.Ya. Korenblit, E.F. Shender, Sov.Phys.JETP62, 1030 (1985)
[10] E. Vincent, J. Hammann, M. Ocio, L. Cugliandolo, in Sitges Conf. on Glassy Systems, ed. M. Rubí, Springer-Verlag, 1997
[11] A.Chudnovskiy, PhD thesis, Würzburg (1998)
[12] K. Hui, A.N. Berker, Phys.Rev.Lett.62, 2507 (1989)
[13] A. Falicov, A.N. Berker, Phys.Rev.Lett.76, 4380 (1996)
[14] O. Nagai, T. Horiguchi, S. Miyashita, in *Magnetic systems with competing interactions*, ed. H.T. Diep, 1994, WorldScientific Publishing Co.